© 2015. Published by The Company of Biologists Ltd | Journal of Cell Science (2015) 128, 900–912 doi:10.1242/jcs.157974

RESEARCH ARTICLE

N-cadherin negatively regulates collective *Drosophila* glial migration through actin cytoskeleton remodeling

Arun Kumar[1,2,3,4,*], Tripti Gupta[1,2,3,4,§], Sara Berzsenyi[1,2,3,4,‡,§] and Angela Giangrande[1,2,3,4,¶]

ABSTRACT

Cell migration is an essential and highly regulated process. During development, glia cells and neurons migrate over long distances – in most cases collectively – to reach their final destination and build the sophisticated architecture of the nervous system, the most complex tissue of the body. Collective migration is highly stereotyped and efficient, defects in the process leading to severe human diseases that include mental retardation. This dynamic process entails extensive cell communication and coordination, hence, the real challenge is to analyze it in the entire organism and at cellular resolution. We here investigate the impact of the N-cadherin adhesion molecule on collective glial migration, by using the *Drosophila* developing wing and cell-type specific manipulation of gene expression. We show that N-cadherin timely accumulates in glial cells and that its levels affect migration efficiency. N-cadherin works as a molecular brake in a dosage-dependent manner, by negatively controlling actin nucleation and cytoskeleton remodeling through α/β catenins. This is the first *in vivo* evidence for N-cadherin negatively and cell autonomously controlling collective migration.

KEY WORDS: Collective migration, glial cells, N-cadherin, actin cytoskeleton, *Drosophila*

INTRODUCTION

Collective migration of neurons and glia cells (clusters, chains, streams and sheets: (Berzsenyi and Giangrande, 2010; Gilmour et al., 2002; Gupta and Giangrande, 2014; Klämbt, 2009; Lemke, 2001; Marín et al., 2010; Rørth, 2003; Valiente and Marín, 2010) implies complex and dynamic cell interactions.

Adhesion molecules play an important role in collective events (Schwabe et al., 2009; Silies and Klämbt, 2010a; Togashi et al., 2009). The cadherin family of Ca^{2+}dependent cell adhesion molecules are primarily involved in homophilic interactions (Arikkath and Reichardt, 2008; Giagtzoglou et al., 2009; Kiryushko et al., 2004) and are required for cell polarity, adhesion and motility (Harris and Tepass, 2010). In the vertebrate and in the *Drosophila* nervous systems, the most abundant classic cadherin is the neural (N)-cadherin (N-cad) (Fung et al., 2008; Stepniak et al., 2009), which promotes the formation of rather small adherens junctions (AJs) and is thought to provide the mechanical basis for static tissue organization (e.g. defined cell arrangement in polarized epithelium) as well as for plastic connections between cells. N-cad has been extensively studied in the context of individual and collective cell migration; however, its precise role is still debated (Asano et al., 1997; Asano et al., 2000; Foty and Steinberg, 2004; Hegedüs et al., 2006; Rappl et al., 2008; Utsuki et al., 2002). Typically, N-cad plays a pro-migratory or an inhibiting role, depending on cell type, on approach (*in vivo* versus *in vitro*, 2D versus 3D assays) and on type of migration. N-cad is necessary in the developing cerebellum of the zebrafish, where it seems to promote differentiation as well as migration of the granule cells (Rieger et al., 2009). However, N-cad expression negatively controls the invasive behavior of gliomas (Péglion and Etienne-Manneville, 2012). The best conditions to understand the relevance of this pleiotropic molecule are the *in vivo* analyses of conditional mutants. For these reasons, we decided to work on a specific type of collective migration called chain migration by using the simple *Drosophila melanogaster* model. Glia cells in the developing wing migrate over the sensory nerve in a chain-like manner. Each member of this cell community is in contact with the neighboring cells, and glia–glia interactions tightly control migration extent, efficiency and coordination (Aigouy et al., 2004; Aigouy et al., 2008; (Berzsenyi et al., 2011). In *Drosophila*, N-cad controls growth cone guidance and axon bundle fasciculation (Iwai et al., 1997); however, it had been suggested that N-cad is not expressed in glia cells (Fung et al., 2008; Iwai et al., 1997). Here, we show that N-cad is dynamically and uniformly expressed in wing glial cells, and that it is necessary for the timely and efficient migration of the chain along the axon bundle. Glial-specific N-cad overexpression severely slows down the initiation of chain migration without affecting the number of AJs. Accordingly, N-cad downregulation triggers the opposite phenotype. Increased N-cad in glial cells enhances the accumulation of β-catenin (β-cat) and α-catenin (α-cat), which has been shown to control actin dynamics by preventing actin nucleation (Shapiro and Weis, 2009). As a consequence, fewer and less-dynamic filopodia are formed in the glial chain. Furthermore, increasing the levels of CYFIP (officially known as Sra-1), a member of the WAVE/SCAR actin nucleation complex, counteracts the effects of N-cad overexpression on glial migration and on actin dynamics. Our *in vivo* study here clarifies the role of N-cad in collective migration and helps to understand the impact of this molecular pathway in morphogenesis and cancer metastasis (Berx and van Roy, 2009; Stepniak et al., 2009).

RESULTS

N-cad is expressed in the *Drosophila* peripheral glial cells

At the anterior margin of the developing *Drosophila* wing, glial cells form a migratory chain along the so-called L1 sensory nerve

[1]Institut de Génétique et de Biologie Moléculaire et Cellulaire, Illkirch, France. [2]Centre National de la Recherche Scientifique, UMR7104, Illkirch, France. [3]Institut National de la Santé et de la Recherche Médicale, U964, Illkirch, France. [4]Université de Strasbourg, Illkirch, France.
*Present address: Department of Entomology, University of California, Riverside, California 92521, USA. ‡Present address: BioTalentum Ltd, Gödöllö 2100, Hungary.
§These authors contributed equally to this work

¶Author for correspondence (angela@igbmc.fr)

Received 21 July 2014; Accepted 17 December 2014

Journal of Cell Science

Journal of Cell Science (2015) 128, 900–912 doi:10.1242/jcs.157974

and move towards the central nervous system (CNS) (Fig. 1) (Giangrande et al., 1993; Murray et al., 1984; Van De Bor et al., 2000). The chain starts moving at ~18h after puparium formation (hAPF) and completes migration by 29 hAPF, upon reaching the proximally located radius glia (Berzsenyi et al., 2011). These glia are in contact with each other and need to interact, suggesting a role for cell adhesion molecules. We, therefore, analyzed the developmental profile of N-cad expression in wing glia (Fig. 1A-M) by using the *repoGal4*glial driver and a UAS GFP reporter (hereafter referred to as *repo >GFP*). N-cad starts being expressed in glial cells at around 17 hAPF (Fig. 1A,B) – just before glia start moving from distal to proximal regions (Fig. 1I) (Aigouy et al., 2004) – and continues to be expressed until the end of migration (29–30 hAPF) (Fig. 1A-H, see white arrows and arrowheads, and red arrowheads in the color-coded panels B′,D′,F′,H; supplementary material Fig. S1A). N-cad seems evenly distributed in the glial cells and is present all along the L1 chain (Fig. 1; supplementary material Fig. S1B,C). In addition, it also accumulates in the axons throughout development (Fig. 1, white and black asterisks).

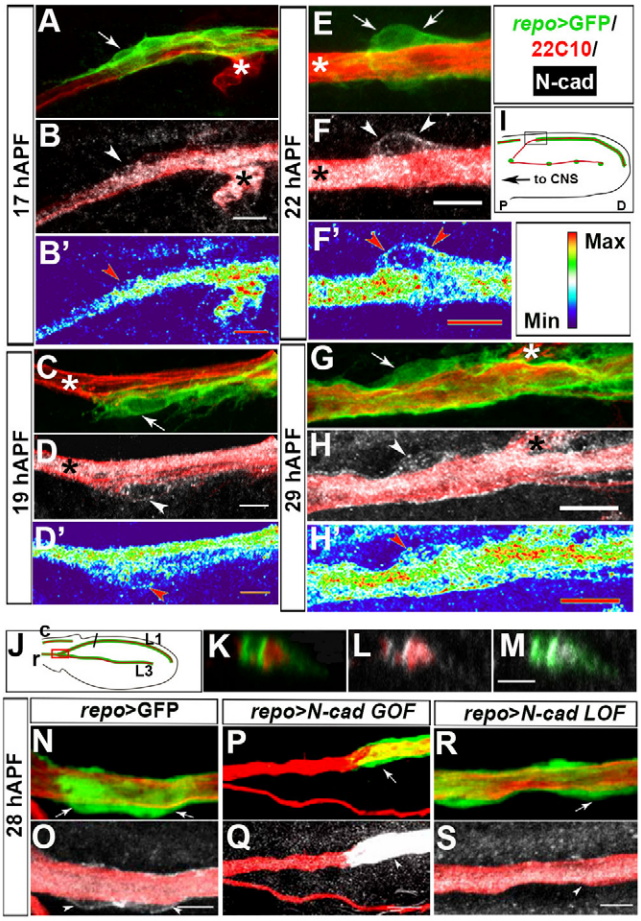

Fig. 1. Expression of N-cad in wing glia during development. (A-H′) Wings at different stages, immunolabeled with anti-22c10 to stain neurons (red), anti-N-cad (white) and anti-GFP (glial cells, green) in the transgenic line *repo >UAS PHGFP* (*repo >GFP*). Maximum confocal projections are shown in all figures, unless otherwise specified. Arrows indicate the glial cells, arrowheads (white and red) the glial N-cad labeling. White asterisks indicate neurons, black asterisks the N-cad signal in those cells. Panels B′,D′,F′ and H′ are the heat maps showing the N-cad expression levels from minimum (dark blue) to maximum (red). By 17 hAPF N-cad starts to accumulate in glia cells, which becomes more prominent at later stages (I,J) Schematic drawings of wings at 19 hAPF (I) and 29 hAPF (J). Neurons are in red, glia in green. c, costa; r, radius nerve; L1 and L3, L1 and L3 nerves (Murray et al.,1984); P and D, proximal and distal regions, respectively. (I) Inset indicates the region shown in panels (A-F′). Inset in J indicates the region shown in G-H′. (K-M) Single optical *z*-cross section of the L1 nerve at 29 hAPF, taken at the position shown in J, immunolabeling and genotypes as above. (N-S) N-cad expression (white arrowheads) in 29 hAPF wing glia (white arrows) of the following genotypes: (N,O) *repo >GFP* (control), (P,Q) *repo >N-cad GOF* and (R,S) *repo >N-cad LOF*. Note the elevated glial N-cad levels in *repo >N-cad GOF* and the reduced N-cad glial levels in *repo >N-cad LOF* compared to those found in *repo >GFP*. Scale bars: 5 µm (A-D′, K-M), 10 µm (E-H′), 5 µm (N-S).

Further, we found that the other abundant AJ-forming cadherin, E-cadherin, is neither expressed by wing glia or neurons (supplementary material Fig. S1D-F) nor does it affect glia migration upon downregulation (supplementary material Fig. S1G). Absence of E-cad and abundance of N-cad suggests that N-cad plays a crucial role in migratory wing glia.

The levels of N-cad affect migration efficiency

Because the expression of N-cad is not restricted to glia, we specifically modified N-cad levels in these cells by using the *repo >*driver and established a protocol in which we to compare glial migration efficiency in different genetic backgrounds. For each genotype, we dissected $n \geq 40$ pupae and compared the percentage of wings that displayed completed glial migration to that observed in control wings (*repo >*GFP). This value, which we define as the migratory index, provides a quantitative estimation of migration efficiency. To score for increased and decreased migration efficiency upon altering N-cad levels, we analyzed a stage at which migration is not fully achieved in control animals and calculated the migratory index by 25 hAPF (Fig. 2A, light grey column).

First, we overexpressed N-cad (gain-of-function or GOF: *repo >N-cad GOF*), upon crossing *UAS N-cad* flies with the *repo >GFP* line and verified that this results in a strong increase of N-cad levels in glia (Fig. 1N-Q). N-cad overexpression significantly decreases glial migration efficiency compared to that observed in control wings (Fig. 2B-G,A, light grey and dark grey columns).

When we knocked down *N-cad* using a *N-cad RNAi* transgene (loss-of-function, LOF: *repo >N-cad LOF*) the N-cad signal was lost in glial cells but not in neurons, which also confirms the efficiency of the used *RNAi* transgene (Fig. 1R,S). By counting the number of *repo >N-cad LOF* wings showing completed glial migration, we observed a significant increase in migration efficiency compared to that observed in control wings (Fig. 2A, red column). Importantly, when we co-expressed the *UAS N-cad* and the *UAS N-cad RNAi* transgenes (*repo >N-cad GOF & LOF*), migration efficiency was restored to control levels, confirming that N-cad overexpression has a regulatory role and that the RNAi effects are specific (Fig. 2A, grey/red striped column).

Glial cells proliferate as they move; therefore, their number increases over the migratory period and cell death occurs only occasionally (Aigouy et al., 2004). To assess whether *N-cad* overexpression also affects the number of glia – which may, in turn, indirectly affect glial migration – we used the panglial nuclear marker Repo (Halter et al., 1995; Xiong et al., 1994) and counted the cells present along the L1 nerve of control and *repo >N-cad GOF* wings at 29 hAPF. N-cad overexpression does not alter the number of glia (control: 90±6 cells; *repo >N-cad GOF*: 85±10 cells, $n=5$, $P=0.42$), indicating that the migratory phenotype

Journal of Cell Science (2015) 128, 900–912 doi:10.1242/jcs.157974

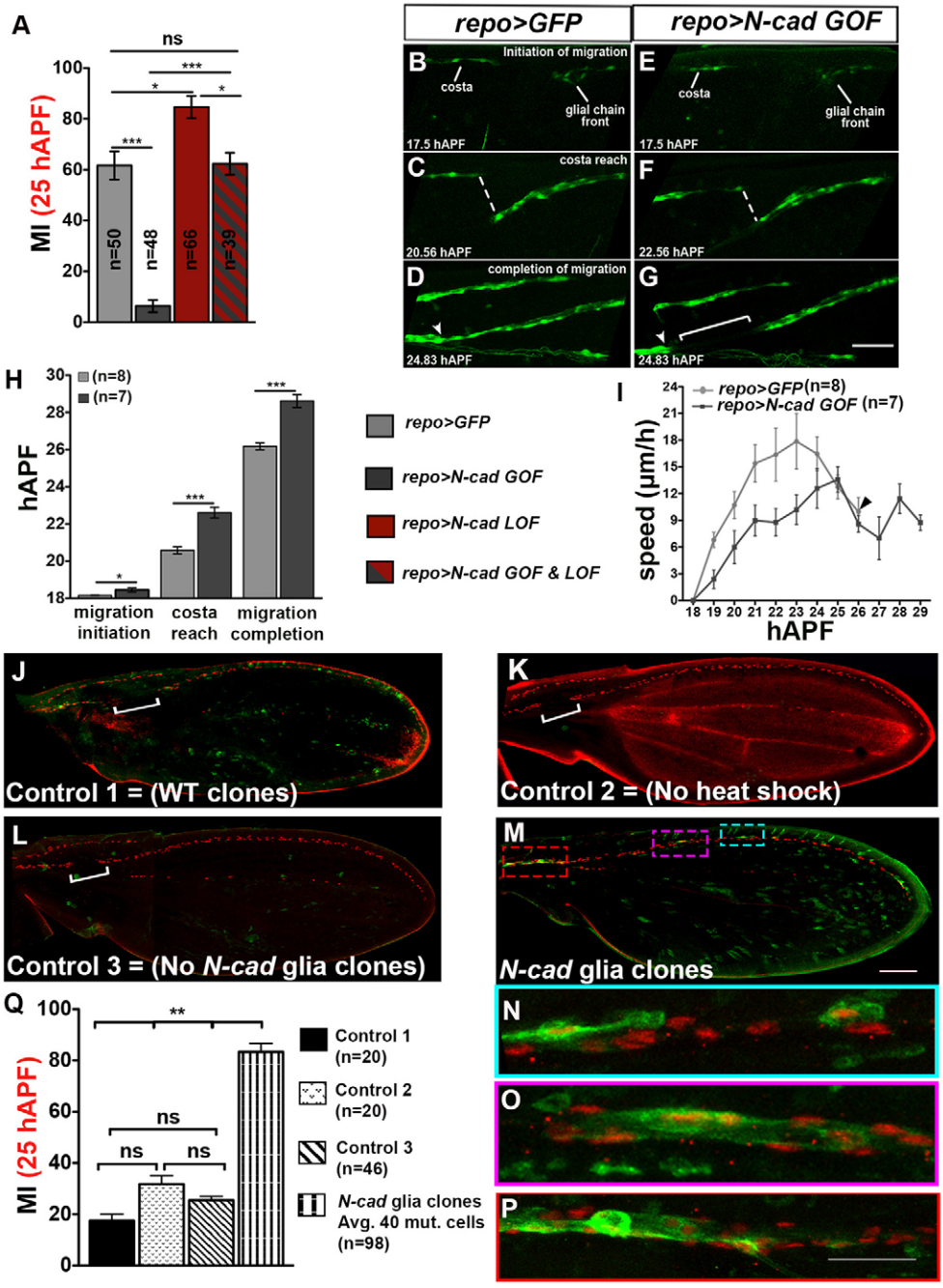

Fig. 2. See next page for legend.

observed in *N-cad GOF* wings is not due to changes in the chain size. We next asked whether N-cad acts cell autonomously in glial migration by analyzing the morphology of the axons in *repo >N-cad GOF* and *repo >N-cad LOF* wings. Since the axons grow in close proximity to glial cells, the excess or reduction of *N-cad* in glia might influence the navigation of the neuronal processes, which might trigger indirect glial migration defects. We compared the advancement of axon growth in *GOF*, *LOF* as well as in control wings and observed no detectable difference in axon/bundle morphology and organization (supplementary material Fig. S2A-D).

Finally, to further validate the migratory phenotype obtained in the conditional GOF and LOF experiments, we generated 'mosaic analysis with a repressible cell marker' (MARCM) clones (Lee and Luo, 2001) in the developing wing by using a *N-cad*-null allele (Iwai et al., 1997). By 25hAPF, wings carrying *N-cad* mutant clones clearly showed an increase in glial migration efficiency, as observed in *repo >N-cad LOF* wings (Fig. 2J-P, the clones carried on average 40 *N-cad* mutant glial cells on the L1 nerve). This phenotype is not observed in control wings that do not carry mutant clones or that carry clones that do not contain mutant glial cells. The results are quantified in (Fig. 2Q). These observations clearly demonstrate that the glial levels of N-cad specifically affect the efficiency of chain migration.

Journal of Cell Science (2015) 128, 900–912 doi:10.1242/jcs.157974

Fig. 2. Role of N-cad in wing glia during development. (A) Glial cell migration phenotype upon N-cad overexpression (*GOF*) and downregulation (*LOF*) in glia using the *repo >GFP* line; see color coding in panel (H). The migratory index (MI) was calculated by counting the number of wings displaying completed migration (i.e. glial chain reaching the proximally located glia on the radius nerve) by 25 hAPF. (B-G) Snapshots at different stages from time-lapse analyses on *repo >GFP* and *repo >N-cad GOF* wings: (B,E) initiation of migration, (C,F) reaching the level of the costa and, (D,G) completion of migration. Note the gap in the wing overexpressing N-cad (bracket), between the L1 glia and the glia on the radius (arrowhead). In these and in the following panels, the nuclear and cytoplasmic GFP transgenic line (*UAS ncGFP*) was used, unless otherwise specified. (H) Quantification of the migratory behavior of control (light grey) and N-cad-overexpressing glia (dark grey) at the three phases highlighted in (B-G). (I) Graph shows the speed of the most-proximal glial cell of the chain (μm/h, *y*-axis; hAPF, *x*-axis) in control and in N-cad-overexpressing glia. The distance covered by the front cell is measured by analyzing the position of the glial soma. Arrowhead points to the completion of migration in control wings, which takes place slightly earlier *in vivo* than in fixed wings. (J-P). Low and high magnification confocal acquisitions of wings obtained for MARCM analysis. (J) Control 1: wild-type wing carrying wild-type clones in glia and showing incomplete migration at 25 hAPF (here, green cells are wild type like the rest of the wing tissue). Animals for control 1 were obtained by crossing *FRT40A* flies with *y,w,hsFLP; FRT40A,tubPGal80/(CyO,ActGFP); tubPGal4,UASmCD8::GFP/TM6,Tb,Hu* flies. (K) Control 2: *N-cad/+* wing without heat shock (i.e. no clones), which shows incomplete migration at 25 hAPF. (L) Control 3: Control 3 is a composite image to cover the whole wing. *N-cad/+* wing with no mutant clones in glia, also showing incomplete migration at 25 hAPF. (M) *N-cad/+* wing carrying mutant clones in glia (*N-cad* mutant glia are in green). Animals for control 2, control 3 and the *N-cad* glia clones were obtained by crossing *N-Cad^{M19}FRT40A* flies with *y,w,hsFLP;FRT40A,tubPGal80/(CyO,ActGFP);tubPGal4,UASmCD8::GFP/TM6,Tb,Hu* flies. The dashed rectangles (cyan, magenta and blue) indicate the regions enlarged in panels N, O and P, respectively. (Q) Quantitative analysis of the indicated genotypes. The white bracket in panels J-L indicates the gap between the L1 and the radius glia. ***$P<0.0001$; **$P<0.001$; *$P<0.05$; ns, not significant. Bars indicate the +s.e.m.; *n*, the number of samples. Scale bars: 50 μm (B-G, J-M), 80 μm (N-P).

High N-cad levels slow down the migration of the glial chain

To gain insights into the kinetics of glial migration in control wings and in N-cad-overexpressing wings, we followed the chain by time-lapse confocal microscopy. The migratory process was subdivided in three phases (Berzsenyi et al., 2011): the earliest one describes migration initiation; the intermediate one identifies the time at which the glial chain reaches the level of the costa; the latest phase refers to migration completion, upon connection of the chain with the proximal glia located on the radius nerve (Fig. 2B-D). N-cad-overexpressing glia start migrating later than control glia and seem to accumulate a delay in the early migratory phases (see Fig. 2H, initiation of migration and reaching the costa). This delay remains detectable until the late phases of migration. On average, the L1 chain reaches the level of the costa and completes migration 1.3 hours later than the control glia (Fig. 2E-G,H). To further quantify migration efficiency, we determined the average distance covered each hour by the first cell soma at the front of the chain. In control animals, the speed of migration increases progressively until 23 hAPF and, then, slows down until migration completion (Fig. 2I). This late slow phase, suggests that the chain front is able to sense some kind of stop signal(s).

When compared to control wings, glial cells overexpressing *N-cad* move at a lower speed when they begin to migrate but accelerate over time. Interestingly, a late slow phase is still detectable, although it is delayed (25 hAPF, Fig. 2I), supporting the view that the chain front may sense the proximity of target cells and that this process is not affected by N-cad. In sum, these data suggest that appropriate levels of N-cad in glial cells control the initiation and speed of the chain.

Ultrastructure of the wing nerve and glial cells

Cadherins constitute structural components of the AJs (Niessen and Gottardi, 2008), stable structures that ensure cell adhesion. It is, therefore, possible that the number of AJs is affected upon *N-cad* overexpression or downregulation in the glial cells, resulting in altered adhesive properties. This change in the strength of glial adhesion to the neighboring glia and/or to the axons may account for the migratory phenotype we observed in *repo >N-cad GOF* and *repo >N-cad LOF* wings. Thus, we analyzed whether *N-cad* overexpression produces morphological alterations at the ultrastructural level and compared the number of AJs that are present in control, *repo >N-cad GOF* and *repo >N-cad LOF* nerves. The fly wing is composed of two juxtaposed layers of epithelial cells, which are separated at the position of five hemolymph filled 'veins', two of which – L1 and L3 – are innervated (Murray et al., 1984) (Figs 1, 3A′). The L1 nerve bundle is composed of several hundred axons and is wrapped by the glial cytoplasmic processes (Fig. 3A). We analyzed eight control wings and eight N-cad-overexpressing wings (60 sections per genotype), as well as seven control wings and N-cad-downregulated wings (25 sections per genotype), then we calculated the percentage of the sections possessing zero to five AJ(s) between L1 glial cells (Fig. 3B). Overall, N-cad-overexpressing wings show a comparable number of AJs to those of control wings. In addition, 50% of the sections display 1–3 AJs between glial cells upon N-cad downregulation, indicating that AJs are still formed, which is in agreement with the observation that, in this background, the L1 chain does not seem loosened compared to that of wild-type wings. Using the same approach, we counted the number of AJs present between glia and axons, and found no significant difference upon changing N-cad levels either (supplementary material Fig. S3A,B). In sum, the manipulation of N-cad levels affects migration efficiency in the absence of significant AJ defects.

N-cad affects migration through catenins

The above data prompted us to analyze the impact of N-cad overexpression on intracellular signaling. One of the key factors associated with classic cadherins in *Drosophila* are β-catenin (β-cat) or Armadillo (Arm) (Yap et al., 1997). First, we immunolabeled *repo >GFP* control animals with an anti-Arm antibody (Fig. 4A-F). As expected, Arm is expressed in the wing epithelium (Fig. 4B, asterisks). Glial Arm labeling is relatively weak, compared to that of N-cad and could be best visualized at the glial membrane that faces the vein lumen (Fig. 4B,C; double headed arrows and arrowheads). We next analyzed the effects of *N-cad GOF* on Arm in the glial cells. To compare the Arm expression profile and levels in control and *repo >N-cad GOF* glial cells (Fig. 4G-L), we ran the experiments in parallel and used the same confocal parameters (which explains why Arm and N-cad levels seem lower in Fig. 4H,I than in Fig. 4B,C, respectively). Arm accumulates at high levels at the cell membrane in N-cad-overexpressing glial cells (Fig. 4K, double-headed arrows). This is in line with previous data showing that different levels of cadherin at the membrane can regulate the accumulation of β-cat/Arm in the cell (Goichberg et al., 2001; Orsulic et al., 1999). The levels of Arm depend on the N-cad doses, which we verified by using a weaker *repo* >driver (supplementary material Fig. S2E-H, red in E,F indicates high

Journal of Cell Science (2015) 128, 900–912 doi:10.1242/jcs.157974

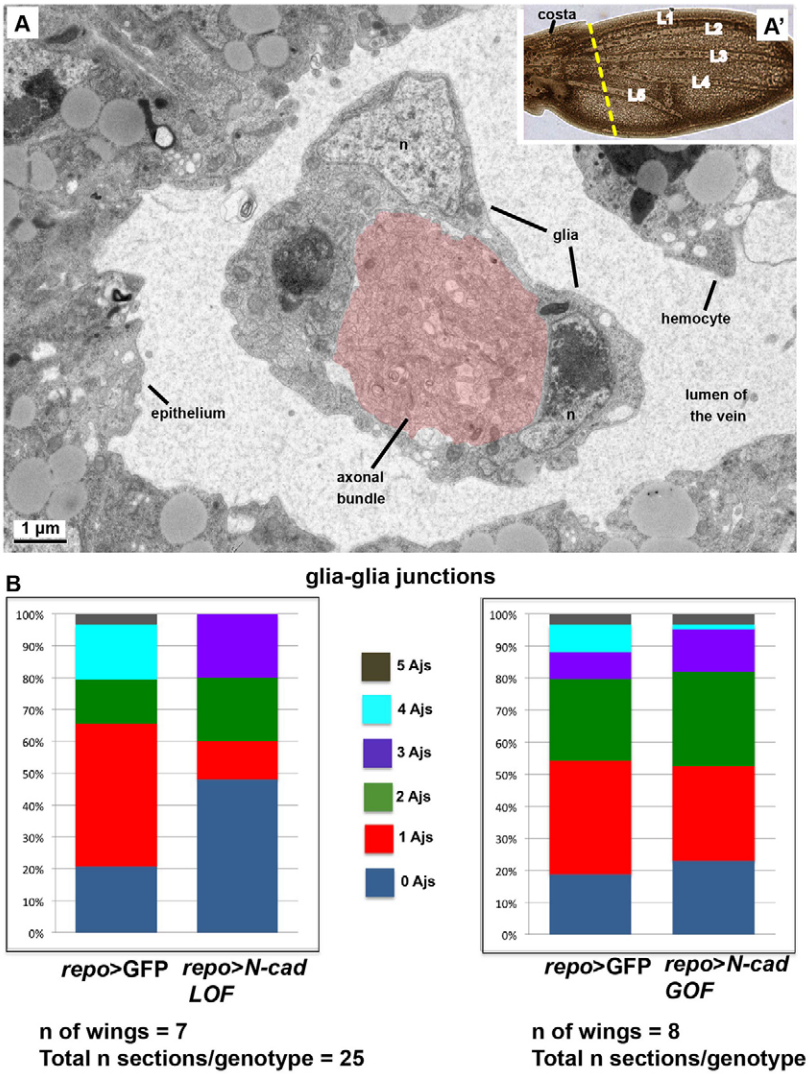

Fig. 3. Ultra-structural analysis of the L1 wing vein. (A) Ultra-thin cross-section of the L1 vein at 29 hAPF at the level of the yellow dashed line indicated in the inset A′. The L1 axonal bundle (pink shading) is surrounded by glial cells. *n*, nuclei of the glial cells. (B) Quantification of the glia–glia AJs in *repo >GFP* (control), *repo >N-cad LOF* and *repo >N-cad GOF* L1 cross-sections. L1 to L5 indicate the five veins present on the wing blade.

levels of Arm). These data strongly suggest that the N-cad-mediated phenotypes involve Arm.

Arm also acts in Wnt/Wg signaling and can be detected at the cell membrane as well as in the cytoplasm and in the nucleus, where it functions as a transcription cofactor (Pai et al., 1997; Peifer et al., 1994). Its actual localization and concentration within the cell eventually defines which function of β-cat/Arm dominates, because cell membrane localization links Arm to the cadherins, whereas cytoplasmic and nuclear localizations links it to Wnt/Wg signaling. The fact that glial cells do not show nuclear accumulation of Arm (Fig. 4A-F and data not shown), suggests that Wg signaling is not very prominent upon *N-cad* overexpression. Nevertheless, to clarify the mode of action of Arm in collective migration, we overexpressed it in glial cells, which leads to its strong accumulation in the nucleus (compare Fig. 4M,N with Fig. 4J,K). Interestingly, under these conditions, glial migration efficiency is similar to that of control wings both at early and late stages (Fig. 4O,P). Thus, the migratory effects of N-cad overexpression seem not associated to Wg signaling.

Drosophila N-cad is a multi-domain transmembrane protein whose extracellular region contains 16 cadherin repeats and whose intracellular part consists of a juxtamembrane domain and an Arm-binding domain. To clarify the mode of action of N-cad, we overexpressed a construct in which the Arm binding domain is deleted (*N-cad ΔArm*) (Yonekura et al., 2007) (Fig. 5A) under the control of the *repo* >driver. Whereas overexpression of the full-length *N-cad* transgene triggers high levels of N-cad and Arm (Fig. 5E-G, arrowhead and double-headed arrow, respectively), overexpression of the *N-cad ΔArm* transgene results in high levels of N-cad but normal levels of Arm (compare Fig. 5B-D with Fig. H-J). Moreover, overexpressing *N-cad ΔArm* in glia does not affect migration efficiency (Fig. 5K). We conclude that the cytoplasmic domain of N-cad participates in regulating glial cell migration via Arm.

β-cat binds α-cat, the main mediator between cadherins and actin that is able to bind both β-cat and actin molecules (Drees et al., 2005) (Rimm et al., 1995). As α-cat provides a bridge between the cell membrane and the cytoskeleton (Benjamin and Nelson, 2008), we analyzed the impact of this molecule onto migration and its genetic interaction with N-cad. Overexpression of α-catGFP fusion protein in glia (*UAS α-catGFP* transgene (Caussinus et al., 2008), Fig. 6A) delays migration (Fig. 6G, compare blue with light-grey column), which is rescued by downregulation of *N-cad* in the same background (*α-catGFP GOF*, *N-cad LOF*, Fig. 6C,D,G, red/blue-striped column). These findings are in line with the observation that *N-cad LOF* accelerates migration (Fig. 6G, red column). Furthermore,

Journal of Cell Science (2015) 128, 900–912 doi:10.1242/jcs.157974

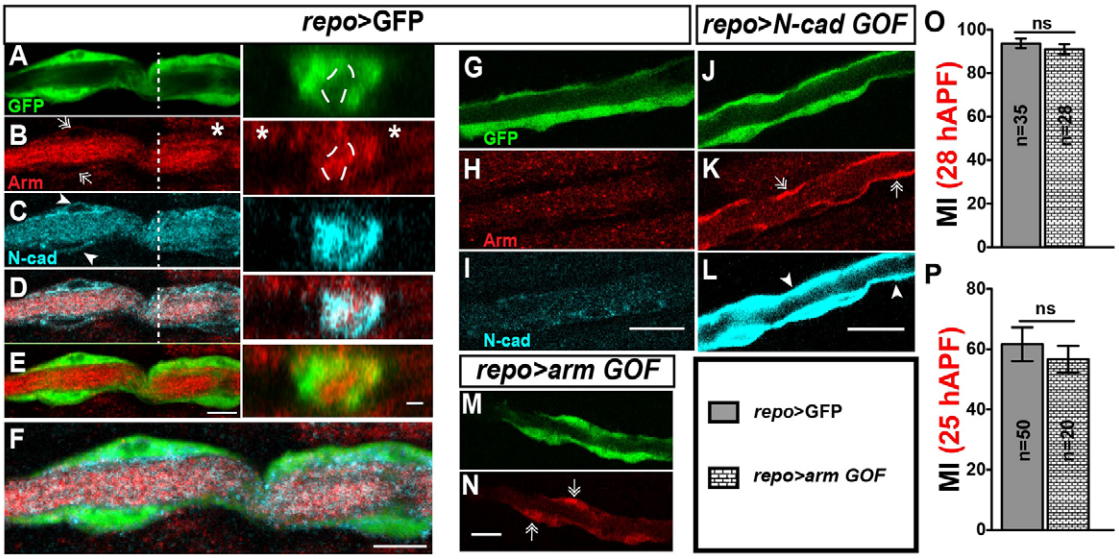

Fig. 4. Expression of Arm and its role in glia migration. (A-F) 29 hAPF *repo >GFP* wings labeled for GFP (green), Arm (red) and N-cad (cyan). Double-headed arrows and arrowheads show Arm (B) and N-cad (C) accumulation on glial membranes, respectively. Dashed line indicates the position of the cross-section shown in the right panels (A-E). (D) Merge of panels B and C. (E) Merge of panels A and B. (F) Merge of panels A,B and C. Arm is also localized in the wing epithelial cells (B, asterisks). (G-L) Comparison of Arm labeling in control and *N-cad GOF* glial cells. (J-L) Arm accumulates at high levels at glial membranes of a *N-cad GOF* wing (K). Note that the acquisition in these control and overexpressing wings was done under the same conditions and at much lower laser intensity compared to that used in panels A-F, which would have led to a saturated signal in N-cad-overexpressing wings. (M,N) *arm GOF* 25 hAPF wing showing nuclear localization of Arm. (O,P) Graphs show the migratory index (MI) upon Arm overexpression in glial cells compared to that observed in *repo >GFP* (control) animals at late and early stages. Note that in the following figures 5-7, the migratory index was analyzed at only 28 hAPF. Scale bars: 5 µm (A-F), cross-sections: 1 µm; 10 µm (G-L, M,N).

overexpressing *α-catGFP* in a *UAS N-cad* background (*α-catGFP GOF*, *N-cad GOF*, Fig. 6E-G grey/blue-striped column) aggravates the N-cad overexpression phenotype (*N-cad GOF*, Fig. 6G, dark-grey column). Finally, decreasing the levels of α-cat in a *UAS N-cad* background rescues the migratory delay induced by N-cad overexpression (*N-cad GOF, α-cat LOF*, Fig. 6G, grey/pink-striped column). Such genetic interactions confirm that α-cat and N-cad work in the same pathway and act in the same direction, to slow glial chain migration.

Finally, and in agreement with the migratory phenotypes, the levels of α-cat are affected by N-cad, as shown by immunolabeling and western blot analyses. GFP was used to monitor α-cat expression in flies that carry the gene fusion *α-catGFP*. The levels of the GFP increase in those animals that also overexpress N-cad (*α-catGFP GOF N-cad GOF*) and decrease in animals that express low levels of N-cad (*α-catGFP GOF, N-cad LOF*) (Fig. 6A-F see arrowheads, S2J). Interestingly, we did not observe a significant difference in *α-cat* mRNA levels in *repo >α-catGFP GOF*, *N-cad GOF* or *N-cad LOF* backgrounds compared to those observed in the control *repo >α-catGFP GOF* animals (supplementary material Fig. S2I). The change in protein but not in RNA levels indicate that N-cad regulates α-cat post transcriptionally, perhaps by stabilizing the protein. Thus, the levels of α-cat change according to Arm in response to different N-cad levels through a post-transcriptional process.

Rescue of actin cytoskeleton remodeling restores glial migration

It has been proposed that, at high levels of cadherin, α-cat accumulates at the membrane, hence increasing the pool of α-cat molecules (Benjamin and Nelson, 2008). As a consequence, α-cat homodimers form and bind actin filaments, thereby preventing the activity of the ARP2/3 complex (Drees et al., 2005). The latter is known to nucleate the branched actin filaments at the cell leading edge and to promote migration (Rotty et al., 2013). Thus, the migratory phenotype induced by altered N-cad levels may be due to defects in the actin nucleation pathway.

Nucleating complexes such as WAVE/SCAR, of which the CYFIP/Sra1 (CYFIP) adaptor is an integral member, activate the ARP2/3 complex (Blagg and Insall, 2004; Stradal et al., 2004). To further validate the hypothesis that N-cad levels control cell migration by preventing appropriate actin cytoskeleton dynamics, we asked whether over-activation of the WAVE/SCAR complex counteracts the defects induced by high levels of N-cad. Indeed, glial migration efficiency is completely rescued in wings that overexpress both CYFIP and N-cad (Fig. 7A, compare green/grey-striped column with dark-grey and light-grey columns). This is also in line with CYFIP acting downstream of N-cad. In addition, downregulation of CYFIP in *repo >N-cad GOF* animals aggravates the migratory defect observed in wings that overexpress N-cad alone (Fig. 7A, compare grey/blue-striped column with dark-grey column). Downregulation of CYFIP in an otherwise wild-type background only slightly reduces migration efficiency (Fig. 7A, compare blue with light-grey column), suggesting that CYFIP is not present in limiting amounts, in agreement with the finding that overexpressing CYFIP in an otherwise wild-type background has no effect on glial cell migration (Fig. 7A, compare green with light-grey column).

To further validate our data, we analyzed the genetic relationship between CYFIP and N-cad using a mutant $CYFIP^{\Delta 85.1}$-null allele (Schenck et al., 2003). Because CYFIP is widely expressed and required, its complete lack is lethal. However, previous data have demonstrated that heterozygous (*CYFIP het*) animals already show mutant phenotypes (Schenck

Journal of Cell Science (2015) 128, 900–912 doi:10.1242/jcs.157974

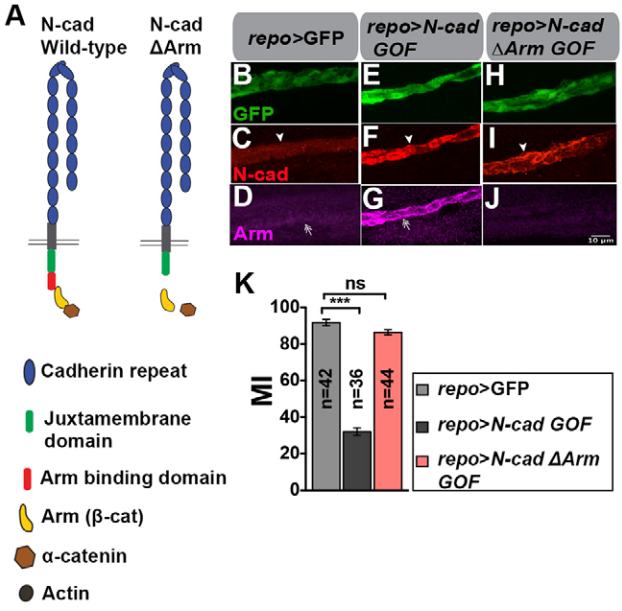

Fig. 5. Deletion of the Arm binding domain of N-cad and the effect of it. (A) Illustration of wild-type N-cad (left) and the *N-cad ΔArm* construct in which the Arm-binding domain is deleted. (B-J) Immunolabeling for GFP (green), N-cad (red) and Arm (magenta) in control wings and in wings overexpressing the *N-cad* transgenes (*N-cad* full-length and *N-cad ΔArm*) under the *repo* >driver. *N-cad GOF* glia display elevated N-cad and Arm levels (compare arrowhead and double-headed arrow in F,G and C,D), whereas in *N-cad ΔArm GOF* glia no Arm can be detected (J). (K) Glial migratory index (MI) in the indicated genotypes. Scale bar: 10 μm (for B-J).

et al., 2004) and we, indeed, found that *CYFIP het* reduces migration efficiency without reducing the number of glial cells (Fig. 7B, yellow column), allowing us to extend the genetic interaction analyses. We reasoned that, if downregulation of N-cad enhanced migration efficiency by enhancing actin nucleation, *CYFIP het* animals that express low levels of N-cad would show an attenuated phenotype. Indeed, in *CYFIP het*, *repo >N-cad LOF* wing glia migrate like in the control wings (Fig. 7B, compare red/yellow striped column with yellow column), although they still differ from glia that only express low levels of N-cad (Fig. 7B, compare red/yellow-striped column with red column), which may have several explanations. For example, CYFIP-independent pathways might also be active or removing one copy of *CYFIP* gene might not be enough to compensate for the vast excess of CYFIP available following knockdown of N-cad. The data that stem from using the *CYFIP*-null allele, nevertheless confirm the hypothesis that N-cad counteracts actin cytoskeleton remodeling, which was further validated by analyzing *CYFIP het*, *repo >N-cad GOF* wings. As predicted from the conditional mutant backgrounds, removing one copy of *CYFIP* aggravates the migratory phenotype triggered by increasing N-cad levels (Fig. 7B, compare grey/yellow-striped column with Fig. 7A dark-grey column). The phenotype is even stronger than that obtained with *CYFIP RNAi*, perhaps because in the latter case *CYFIP* is only downregulated in glia (Fig. 7B, compare grey/yellow-striped column with grey/blue-striped column). All together, these data show that CYFIP plays an important role in the N-cad cascade affecting collective migration.

Finally, we investigated the different migratory phases by using time-lapse confocal microscopy in order to analyze the kinetics of the *N-cad CYFIP* interactions *in vivo*. At all stages, migration efficiency is similar in wings overexpressing both N-cad and CYFIP compared with control wings (Fig. 7C, compare light-grey with green/grey-striped columns). In contrast, overexpressing N-cad alone results in delayed migration in all phases (Fig. 7C, compare dark-grey with light-grey columns). Overexpressing CFYIP progressively rescues N-cad overexpression: at the initiation phase, it mildly improves the migratory defect induced by N-cad overexpression and the rescue becomes more effective at later phases (Fig. 7C, compare dark-grey with green/grey-striped columns, initiation phase: $P=0.132$; reaching the costa nerve: $P=0.002$; completion of migration: $P=0.0003$). As expected, downregulation of N-cad accelerates all phases of migration (Fig. 7C, compare light-grey with red

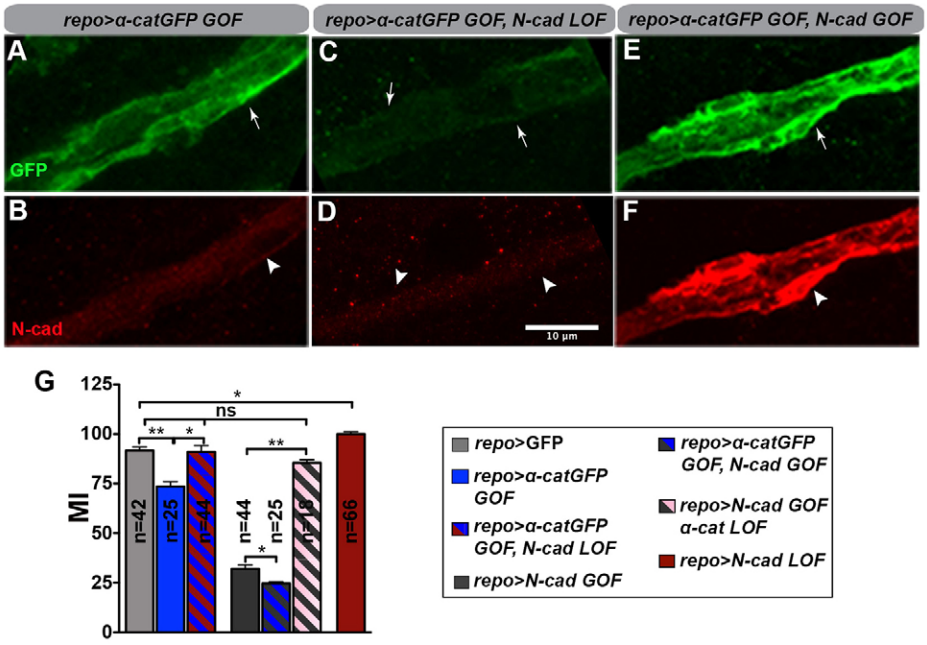

Fig. 6. Distribution and role of α-cat upon *N-cad* gain and loss of function. (A-F) 28 hAPF wings showing α-catGFP (green) and N-cad (red) expression upon *N-cad GOF* and *N-cad LOF* using the *repo >α-catGFP* transgene. Note the reduced amount of GFP *in repo >α-cat GFP; N-cad LOF/+* (C,D) and the elevated levels of GFP in *repo >α-catGFP; N-cad GOF/+* (E,F) glial cells compared to *repo >α-catGFP/+* control wing (A,B). (G) Migratory index (MI) in the indicated genotypes. Scale bar: 10 μm (for A-F).

Journal of Cell Science (2015) 128, 900–912 doi:10.1242/jcs.157974

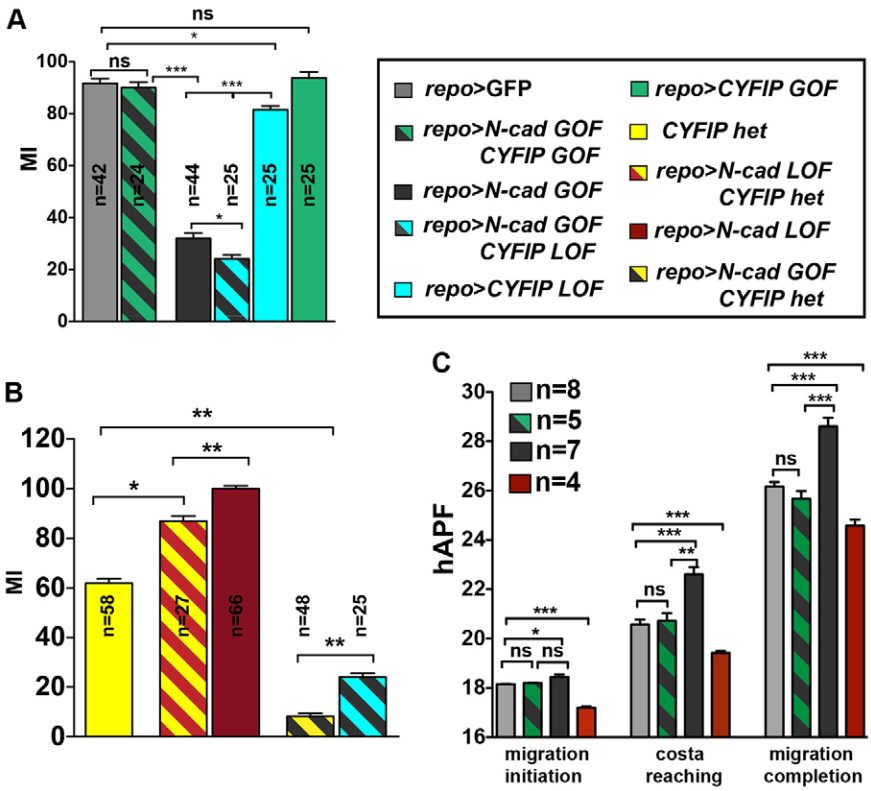

Fig. 7. CYFIP rescues N-cad-mediated migratory defects. (A,B) Migratory index (MI) in the indicated genotypes. (C) Quantification of the migratory behavior at the three phases in the indicated genotypes.

columns). In sum, promoting actin nucleation counteracts the effects of high N-cad levels during collective migration.

N-cad affects actin cytoskeleton remodeling

The above data highlight the role of N-cad in signaling to α-cat and indicate that the migratory phenotypes depend on actin cytoskeleton defects. To investigate these phenotypes *in vivo*, we followed the organization of the actin cytoskeleton at the stage at which cells start to migrate. We used the *UAS actin42AGFP* transgene under the control of the *repo* >driver and focused on the cells at the front of the chain, where the behavior of filopodia can be more easily scored and is more prominent. Using fast time-lapse confocal microscopy, we analyzed control wings (*repo >actin42AGFP*), N-cad-overexpressing wings (*repo >actin42AGFP; N-cad GOF*), wings that overexpress both N-cad and CYFIP (*repo >CYFIP GOF, N-cad GOF*) and wings that express low N-cad levels *(repo >actin42AGFP; N-cad LOF)*. Filopodia are more static in N-cad-overexpressing than in control glial cells, a phenotype that is rescued when CYFIP is reintroduced (Fig. 8A-C). The most dynamic filopodia are of glial cells that express low levels of N-cad (Fig. 8D).

Next, we quantified two parameters, the number of filopodia and their length, in the four genetic backgrounds. To achieve this, we analyzed the cell somata at the migration front and, for each cell soma, we measured the length of single filopodia as well as the number of filopodia (see graphs in Fig. 8E,F).

The number of filopodia significantly decreases in *N-cad GOF* compared to that observed in control glial cells and the cytoplasmic processes are also considerably shorter in *N-cad GOF* glia (Fig. 8A,B,E,F). Conversely, downregulation of N-cad in glia results in increased filopodia length (Fig. 8D,E). This difference is not due to the number of glia at the front of chain, which does not change in the four indicated genotypes (Fig. 8G).

Quantitative analyses in animals overexpressing both N-cad and CYFIP revealed that the number and the complexity of filopodia are significantly different from those observed upon overexpression of N-cad alone, thus, *CYFIP* rescues the N-cad-overexpression phenotype, at least in part (Fig. 8C,E,F). Panels H and I in Fig. 8 summarize the quantitative data on filopodia length and on the number of filopodia per soma in the indicated genotypes (Fig. 8, H and I).

Taken together, these results show that the levels of N-cad tightly regulate CYFIP-mediated actin cytoskeleton remodeling in migrating glial cells.

DISCUSSION

Cadherins act in many biological processes including collective migration, a dynamic event that involves three-dimensional constraints. To grasp the role and mode of action of cadherins in collective migration, the use of animal models and accurate genetic analyses are of paramount importance. We here show that N-cad is expressed in the glial cells present in the developing wing of *Drosophila* and that it negatively regulates chain migration efficiency by controlling actin dynamics.

N-cadherin and glial migration

Glial cells constitute a highly motile population. They migrate extensively during development and even some adult glial cells do so: astrocytes in the mammalian brain, for example, migrate to lesions caused by injury or neurodegeneration, a process commonly known as reactive astrogliosis (Sofroniew and Vinters, 2010). Tumor glial cells move through the nerve tissue, leading to formation of glioma, the most aggressive form of cancer in the nervous system (Cayre et al., 2009). In addition, glia of the peripheral nervous system (PNS), such as vertebrate perineurium and Schwann cells (Klämbt, 2009), as

Journal of Cell Science (2015) 128, 900–912 doi:10.1242/jcs.157974

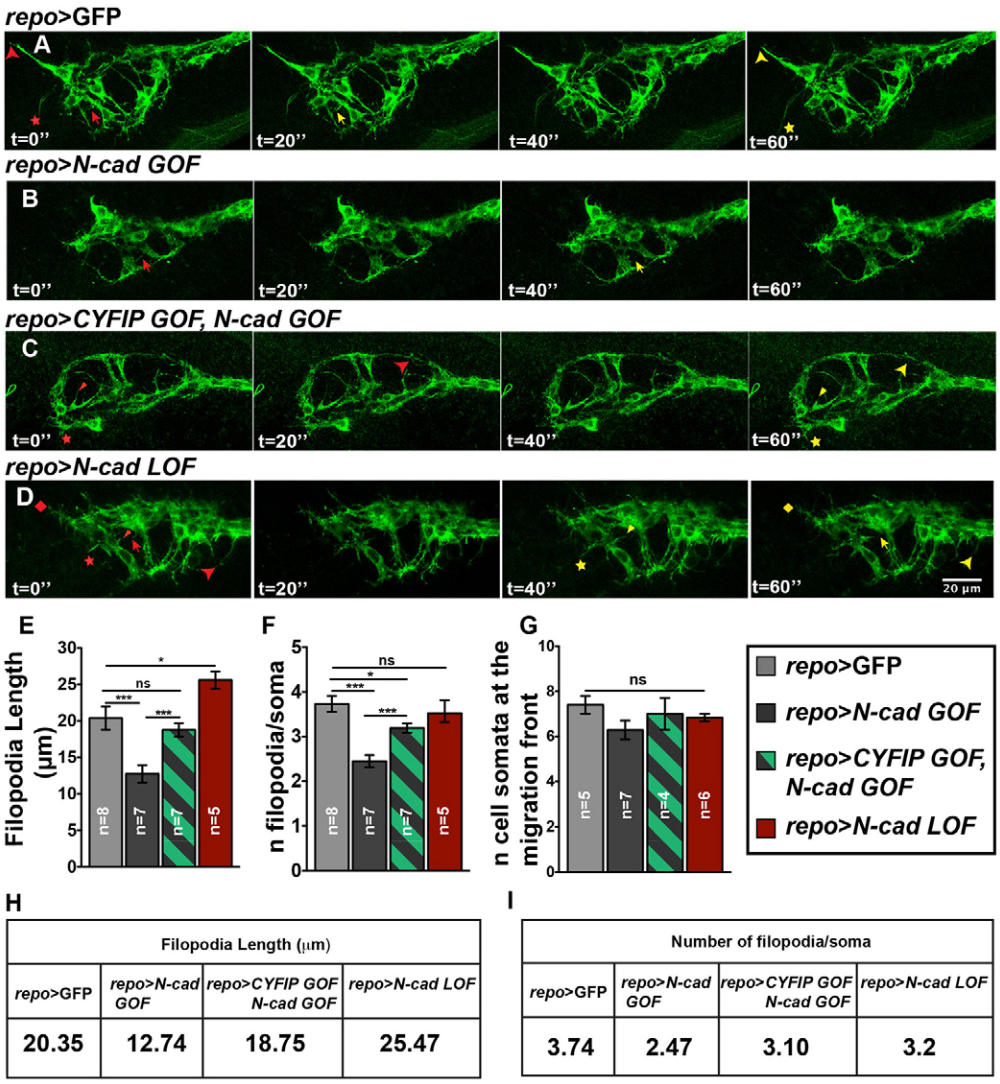

H

Filopodia Length (µm)			
repo>GFP	repo>N-cad GOF	repo>CYFIP GOF N-cad GOF	repo>N-cad LOF
20.35	12.74	18.75	25.47

I

Number of filopodia/soma			
repo>GFP	repo>N-cad GOF	repo>CYFIP GOF N-cad GOF	repo>N-cad LOF
3.74	2.47	3.10	3.2

Fig. 8. N-cad and actin cytoskeleton dynamics. (A-D) Confocal time-lapse images of *Drosophila* wings taken at 20-second intervals that show the organization of glial cytoplasmic processes at the chain front in the following genotypes: *repo >GFP* (control); *repo >N-cad GOF*; *repo >CYFIP GOF N-cad GOF* and *repo >N-cad LOF*. Red arrows, triangles, square and stars indicate the initial shape and position of the filopodium, symbols in yellow show the same filopodium upon reorganization. (E) Quantification of filopodia lengths (in µm) at initiation of migration in all genotypes. (F) Number of filopodia present per cell soma in the indicated genotypes. (G) Number of cell somata present at the migration front. (H,I) Summaries of the data shown in panels E and F. Scale bar: 20 µm (for A-D). Note that the *UAS Actin42A GFP* line was used in this figure to follow actin dynamics.

well as embryonic and pupal *Drosophila* and *Manduca* glia, move as collectives to reach their final destination (Cafferty and Auld, 2007; Klämbt, 2009; Koussa et al., 2010; Silies and Klambt, 2010a; von Hilchen et al., 2008; von Hilchen et al., 2013). This makes glia a valuable tool to analyze the role of cadherins in cell migration in the nervous system. In contrast to previous reports (Fung et al., 2008; Iwai et al., 1997), we found that N-cad is expressed in peripheral glia and is required for their migration.

N-cad negatively controls the glial migratory process, its levels modulating migration initiation and speed. In line with the findings that N-cad stays on after migration has ended and that its overexpression delays rather than stops migration, N-cad has a permissive rather than instructive role. We propose that timely expressed pro-migratory cues trigger the movement of the chain, and that N-cad fine-tunes the process by acting as a brake. N-cad is, therefore, part of the network that controls the efficiency of collective migration. Interestingly, N-cad is expressed in embryonic PNS (supplementary material Fig. S4A,B, arrowheads) but not in CNS glia cells (supplementary material Fig. S4C), which seem to move mostly as single cells (Klämbt, 2009).

In summary, whereas N-cad is known to be present in vertebrate PNS glia during development and in pathological conditions this is, to our knowledge, the first *in vivo* report on its cell-specific role in glial migration.

N-cadherin and collective migration

Border cells in the *Drosophila* ovary have been extensively studied as a model for collective migration and they depend on E-cad to migrate (Godt and Tepass, 2009; Montell, 2003; Rørth, 2009). Moreover, it has been recently shown that border cells that express low levels of E-cad protrude less than wild type cells and fail to follow their migratory pathway (Cai et al., 2014; Montell et al., 2012). Thus, E-cad acts positively on border cell migration and on directional sensing. We propose that the opposite roles of E-cad in border cells and N-cad in glial cells reflect the different organization and migratory strategies of the two ‘collectives’. Border cells move as a compact cluster and present features of apico-basal polarity; cells in the glial chain, instead, show less-tight contacts with each other (supplementary material Fig. S4D,E) and do not display apico-basal polarity. Thus, whereas border cells move like a patch of epithelial cells, glia cells show a behavior that is more similar to that of mesenchymal cells. The size and shape of the collective significantly differs as well, and one or two border cells are sufficient to trigger the migration of the cluster containing 8–12 cells. In contrast, several pioneer glia

Journal of Cell Science (2015) 128, 900–912 doi:10.1242/jcs.157974

cells are necessary to drag the long chain made of 60–70 cells, spanning over almost 800 µm. Moreover, the long glial chain relies on relay mechanisms and homeostatic interactions to migrate efficiently (Aigouy et al., 2004; Berzsenyi et al., 2011). As proposed by Montell and collaborators (Cai et al., 2014), various mechanisms can account for the diversity of morphogenetic movements; therefore, understanding the signaling cascades mediated by cadherins will require the analysis of different collectives (chains, clusters, streams, sheets and tubes, and large versus small migratory communities).

Finally, E-cad and N-cad seem to have different structural properties and are associated with AJs of different size (Chu et al., 2006; El Sayegh et al., 2007; Uchida et al., 1996) (Harris and Tepass, 2010; Tepass et al., 2000). Thus, E-cad may control the tension and asymmetry that are necessary in compact and small migratory groups, whereas N-cad regulates dynamic processes that have a stronger impact on loose and large collectives, actin nucleation providing the required relay mechanisms. It will be interesting to assess the precise role of N-cad in other migratory collectives that show loose contacts.

Cadherins and AJs

Cadherins are habitually regarded as components of the AJs; however, N-cad is widely distributed in wild-type glia cells and altering its protein level affects migration in the absence of significant AJ defects. The number of glia–glia AJs does not change significantly between control and N-cad-overexpressing glia, nor does the structure of the AJs seem to change, suggesting that excessive N-cad levels do not induce the formation of larger AJs with altered adhesive capacity (supplementary material Fig. S3C-F). Similarly, conditional N-cad knockdown does not eliminate AJs. Our results are in line with the finding that cadherin–catenin complexes can be observed all along the cell membrane in MDCK epithelial cells (Näthke et al., 1994). Moreover, *in vitro* assays in which CHO cells or fibroblastic L-cells were used have suggested that cadherins can mediate adhesion between cells that lack zonula adherens AJ structures (Brieher et al., 1996; Nose et al., 1988). These data suggest that cadherins can organize differently, i.e. junctional and non-junctional, hence providing distinct functions. Our data, obtained by using glia cells of the *Drosophila* wing, are in agreement with this hypothesis. The assembly of N-cad in glial AJs may occur at preferred cell contact points that are more stable or serve as anchor sites for cell translocation. The rest of diffusely distributed cadherin/catenin complexes are likely to trigger the formation of more-transient contacts that are important in the push-and-pull process at work in the glial chain.

Immunoprecipitation studies have shown that cis dimers can be formed by cadherins of the same cell (Brasch et al., 2012; Shan et al., 2000; Shapiro and Weis, 2009); however, it is unknown which role such cis interfaces play *in vivo* (Brasch et al., 2012). Since glial cells at the chain front are not in contact with other glial cells on their proximal side, N-cad lateral clustering may occur at that position. A non-mutually exclusive possibility is that N-cad at the chain front interacts with axonal N-cad. Finally, the extracellular matrix (ECM) constitutes another key player in cell migration and interacts with cadherins (for reviews, see Doyle et al., 2013; Weber et al., 2011). Also, integrins in glia have been recently shown to shape the larval *Drosophila* CNS (Meyer et al., 2014). It will be interesting to assess whether and how N-cad and ECM interact in the collective process of glial migration. Although additional work will be necessary to clarify these issues, the present study provides novel hints on the role of N-cad in collective migration.

Cadherin–catenin interaction controls actin dynamics

At their cytoplasmic domains, cadherins are associated with adapter molecules that link cell membrane to actin cytoskeleton dynamics. Cadherin activation by clustering can lead to a change in the arrangement of actin filaments at the cell membrane, which in turn regulates cell shape and migration (Nelson, 2008). A key organizer of actin assembly at the cell membrane is α-cat (Kobielak and Fuchs, 2004; Oda et al., 1993), which has been shown to either bind β-cat as a monomer or the actin filaments as homodimer (Drees et al., 2005; Yamada et al., 2005). Cadherin-dependent accumulation of α-cat below the membrane leads to its dissociation from the cadherin–catenin complex (Drees et al., 2005). This promotes actin bundling and suppresses the branching activity of the ARP2/3 actin nucleation complex, which is crucial for cell migration (Benjamin and Nelson, 2008). Thus, when the amount of cadherin is increased, the continuous assembly of the actin network by the ARP2/3 complex – to which CYFIP belongs – is reduced, and migration is less efficient. Conversely, depletion of cadherin causes a reduction of α-cat at the membrane, hence, enhancing actin branching and cell motility. The migratory phenotypes observed upon glial-specific manipulation of gene expression, the rescue experiments, the quantitative analysis of α-cat mRNA/protein and the *in vivo* analyses of actin dynamics all support this hypothesis. Finally, whereas cadherin overexpression may cause perturbation of Wnt/Wg signaling (Sanson et al., 1996), N-cad-dependent accumulation of Arm at the membrane and the fact that nuclear overaccumulation of Arm does not induce migratory defects, show the importance of N-cad and Arm in the control of actin dynamics. It is interesting to notice that, although cadherins have opposite effects on the migration of border and glia cells, Arm's sole function seems to link them to α-cat (border cells: Pacquelet and Rørth, 2005).

In sum, our *in vivo* investigation supports the hypothesis that classic cadherins control collective migration through remodeling of the actin cytoskeleton, hence, providing a new platform for understanding the molecular signaling cascade underlying this process in physiological and disease conditions.

MATERIALS AND METHODS

Fly stocks and genetics

Flies were raised at 25°C. *repoGal4* (indicated as *repo* >) (from V. Auld, University of British Columbia, Vancouver, Canada) was used to drive glial-specific expression of *UAS ncGFP* (nc indicating nuclear and cytoplasmic) (Aigouy et al., 2008), *UAS mCD8GFP* (m indicating membrane) (Aigouy et al., 2008), *UAS PHGFP* (fusion protein between the pleckstrin homology domain of PLC-δ and the GFP coding sequence) (was from A. Zelhof, Indiana University, Bloomington, Indiana, United States of America) (Zelhof and Hardy, 2004), *elav-DsRed* (Aigouy et al., 2008); *UAS N-cad* (was from T. Uemura, Kyoto University, Kyoto, Japan) (Iwai et al., 2002); *UAS N-cad RNAi* (VDRC stock center) (Cai et al., 2014); *UAS Arm* (Bloomington stock center), *UAS N-cad ΔArm* (was from S. Yonekura, Shinshu University, Nagano, Japan) (Yonekura et al., 2007), *UAS α-catGFP* (was from M. Affolter, Biozentrum, Basel, Switzerland) (Caussinus et al., 2008), *UAS α-cat RNAi* (Bloomington stock center), *UAS Actin42AGFP* (was from J. Casanova, IRB, Barcelona, Spain) (Gervais and Casanova, 2011), *UAS CYFIP* (Schenck et al., 2003), *UAS CYFIP RNAi* (Galy et al., 2011), $CYFIP^{\Delta 85.1}$ (Schenck et al., 2004); *y,w,hsFLP;FRT40A,tubPGal80/(CyO,ActGFP);tubPGal4,UASmCD8::GFP/TM6,Tb,Hu* (was from H. Reichert Biozentrum, Basel, Switzerland) (Bello et al., 2008), $N\text{-}Cad^{M19}FRT40A$ (was from M. Kurusu, National Institute of Genetics,

Journal of Cell Science (2015) 128, 900–912 doi:10.1242/jcs.157974

Shizuoka, Japan) (Kurusu et al., 2012), *FRT40A* (Bloomington stock center). Clones were obtained after a 37℃ 20–30 minute heat-shock at early L3. Note that, in supplementary material Fig. S2I,K a different and weaker *repoGal4* line was used for comparison (B.W. Jones) (Lee and Jones, 2005).

In vivo Imaging

Dissection, time-lapse imaging and immunolabeling were performed as described in (Aigouy et al., 2008; Aigouy et al., 2004; Soustelle et al., 2008). Fast imaging of glial cells was performed using SP5 Leica confocal microscopes equipped with hybrid detectors. The GFP-labeled region in the wing was selected and scanned in the *z*-axis, using the 488 nm laser at 20-second intervals. We avoided photo bleaching by using a low magnification and reducing the exposure time. Since the time defined to quantify filopodium length was short, no reduction in GFP intensity was noticed. Maximum projections for time-lapse movies were obtained using the ImageJ software. Images were annotated using Adobe Photoshop and Illustrator,movies were converted to QuickTime format using ImageJ. Statistical analysis was done using Student's *t*-test; bars indicate standard error of the mean (±s.e.m). For quantitative analyses, distances were calculated manually and then converted into micrometers upon considering the used magnification.

Measuring the length of filopodia

Filopodium length in each of the isolated soma was measured from the surface of the soma to the end of the filopodium by using the ImageJ software (http://imagej.nih.gov/ij/), and is represented in pixels (x). Since we know the size (s) of each pixel (in µm) from the confocal acquisition information panel, we can get the actual length in µm of each of these filopodia by multiplication (x×s).

Electron microscopy

High-pressure freezing

Wings were dissected in cold phosphate buffered saline (PBS) and transferred to flat carriers (200 µm deep, Leica) filled with 20% BSA in PBS (Sigma). Cryo-immobilization was performed in Leica EMPACT-2 high-pressure-freezing apparatus. Freeze substitution was processed in Leica AFS for 60 hours at −90℃ in 1% osmium tetroxide (OsO_4), 0.5% uranyl acetate, 0.5% glutaraldehyde and 2% water in pure acetone. Temperature was slowly raised to −30℃ at a 3℃/hour rate. After 6 hours at −30℃, samples were extensively rinsed with pure acetone and permeated by a graded concentration of epoxy resin Epon 812. When the concentration of the resin reached 70%, the temperature was gradually raised to 20℃. The permeation was then finished by three incubations in pure Epon (2 hours each). Blocks were left for 48 hours at 60℃ for polymerization. Ultra-thin sections (50–0 nm) were collected on carbon/formvar-coated copper slot grids, contrasted with uranyl acetate and lead citrate. Images were acquired using an Orius1000 CCD camera (Gatan) mounted on a Philips CM12 transmission electron microscope operated at 80 kV.

Chemical fixation

The wings were dissected in PBS buffer and immediately immersed in the fixative [2.5% glutaraldehyde and 4% formaldehyde in 0.1 M pH 7.4 phosphate buffer (PB)]. After a minimum fixation time of 2 hours, samples were rinsed with PB and post-fixed for 1 hour in 1% OsO_4 at 4℃. After several rinses in distilled water, samples were gradually dehydrated in acetone (50%, 75%, 90%, 95%, 100%) and permeated with epoxy resin in pure acetone (25, 50, 75 and 100%). The wings were flat-embedded between two sheets of aclar (EMS) as described (Kolotuev et al., 2010) and left to polymerize for 48 hours at 60℃. Targeted ultra-microtomy was used to systematically section the wings in the same region. Ultra-thin sections (60 nm) were collected on electron microscope grids.

Western blot assay

Wing extracts were produced from the following genotypes: (a) *repo >, UAS α-catGFP/+*; (2) *UAS N-cad/+*; *repo >, UAS α-catGFP/+* and (c) *UAS N-cad RNAi/+; repo >, UAS α-catGFP/+*. Protein lysates (30–40 µg) extracted by freeze-thawing cell pellets (in 400 mM KCl, 25 mM Tris HCl pH 7.9, 10% glycerol) were loaded on gradient acrylamide gels (Invitrogen), transferred onto nitrocellulose membrane after electrophoresis and probed with primary antibodies: chicken anti-GFP (ab13970, Abcam, 1:5000) and rabbit anti-actin (A2066 Sigma Aldrich, 1:5000). Signals were detected with Pierce ECL western blot substrate (Thermo Fisher Scientific, Waltham, MA) using horseradish peroxidase (HRP)-conjugated rabbit anti-chicken and goat anti-rabbit (Jackson ImmunoResearch) secondary antibodies (1:10,000). Note that for both western blot and quantitative reverse transcriptase PCR (qRT-PCR) assays ~200 wings were dissected for each mentioned genotype and each experiment. Wings were staged between 20 and 23 hAPF.

Reverse transcription and quantitative reverse transcriptase PCR

Total RNA was analyzed in control wings (*repo >GFP/+*) and in wings of the following genotypes: (a) *repo >, UAS α-catGFP/+*; (b) *UAS N-cad/+*; *repo >, UAS α-catGFP/+* and (c) *UAS N-cad RNAi/+; repo >, UAS α-catGFP/+*. RNA was purified with TriReagent (MRC), reverse transcribed with SuperScriptII reverse transcriptase (Invitrogen) by using a mix of random hexamers (6 µM) and oligodT primers (5 µM), and analyzed by quantitative PCR (qPCR) (Roche LightCycler480) with Syber Green (Roche) Master mix. For each gene, expression levels were automatically calculated (LightCycler480 Software, release 1.5.0) by calibration against gene-specific standard curves generated by input cDNAs. Obtained values, normalized to the against Actin5C, derived from three amplification reactions, each performed in three independent experiments. PCR primers are: *α-cat*(forward): 5′-TGACCAACGTGTA-GGAGCAG-3′, *α-cat*(reverse): 5′-ACTCCGTCGTAAACCAAACG-3′; *actin*(forward): 5′-TCCAGTCATTCCTTTCAAACC-3′, *actin*(reverse): 5′-GCAGCAACTTCTTCGTCACA-3′.

Immunolabeling and antibodies

Staged pupae were fixed in 4% PFA-PBS (paraformaldehyde in PBS) at 4℃ for 2 hours. Pupae were dissected in PBT (PBS + Triton-X100,0.3%). After quick washes in PBT, wings were incubated in PBT-NGS (5% normal goat serum in PBT) for 20 minutes at room temperature on a planar shaker. Then, the samples were incubated overnight with primary antibodies (diluted in PBT-NGS): the panglial mouse anti-Repo antibody (1:800), the neuron-specific mouse anti-22c10 antibody (1:1000) (DSHB7), chicken anti-GFP (1:1000) (Abcam), rat anti-N-cad (1:50-1:100) (DNEx8-DSHB) and mouse anti-Arm (1:50-1:100) (N27A1-DSHB). After three washes in PBT, wings were incubated for 2 hours at room temperature with secondary antibodies raised in mouse coupled to Cy3 and Cy5, in rat coupled to Cy5 and in chicken coupled to FITC, fluorescent dyes were purchased from Jackson Immuno Research Laboratories, diluted 1:500 in PBT-NGS. Following a final wash in PBT, wings were mounted on slides in Aqua-Poly/Mount medium (Polysciences Inc.).

Acknowledgements

We thank Jordi Casanova, Markus Affolter, Venessa Auld, Claude Desplan, Mitsuhiko Kurusu, Heinrich Reichert, Andrew Zelhof, Tadashi Uemura, Shinichi Yonekura, the DHSB and the Bloomington Stock Center for reagents and flies. We thank Celine Diebold and Claude Delaporte, and the IGBMC fly, cell separation and imaging facilities for technical assistance. We thank Yoshi Yuasa and Pierre B. Cattenoz as well as the other members of the lab for valuable input and comments on the manuscript. We also thank Yannick Schwab for help with the EM and all the members of the lab for critically reading the manuscript.

Competing interests

The authors declare no competing or financial interests.

Author contribution

A.K., S.B. and T.G. carried out all the experiments. A.G. created the model. A.K., S.B., T.G. and A.G. analyzed the data and wrote the manuscript.

Funding

This work was supported by INSERM, CNRS, UDS, Hôpital de Strasbourg, ARC, INCA, Indo-French Center for the Promotion of Advanced Research (CEFIPRA) and ANR grants. S.B., A.K. and T.G. were funded by AFM, ARC and CEFIPRA

fellowships, respectively. We also thank The Company of Biologist for providing A.K. with a travelling fellowship to visit the lab of Gerd Technau (Institut für Genetik, Johannes Gutenberg Universität Mainz, Germany). The IGBMC was also supported by a French state fund through the ANR labex.

Supplementary material

Supplementary material available online at
http://jcs.biologists.org/lookup/suppl/doi:10.1242/jcs.157974/-/DC1

References

Aigouy, B., Van de Bor, V., Boeglin, M. and Giangrande, A. (2004). Time-lapse and cell ablation reveal the role of cell interactions in fly glia migration and proliferation. *Development* **131**, 5127-5138.

Aigouy, B., Lepelletier, L. and Giangrande, A. (2008). Glial chain migration requires pioneer cells. *J. Neurosci.* **28**, 11635-11641.

Arikkath, J. and Reichardt, L. F. (2008). Cadherins and catenins at synapses: roles in synaptogenesis and synaptic plasticity. *Trends Neurosci.* **31**, 487-494.

Asano, K., Kubo, O., Tajika, Y., Huang, M. C., Takakura, K., Ebina, K. and Suzuki, S. (1997). Expression and role of cadherins in astrocytic tumors. *Brain Tumor Pathol.* **14**, 27-33.

Asano, K., Kubo, O., Tajika, Y., Takakura, K. and Suzuki, S. (2000). Expression of cadherin and CSF dissemination in malignant astrocytic tumors. *Neurosurg. Rev.* **23**, 39-44.

Bello, B. C., Izergina, N., Caussinus, E. and Reichert, H. (2008). Amplification of neural stem cell proliferation by intermediate progenitor cells in Drosophila brain development. *Neural Dev.* **3**, 5.

Benjamin, J. M. and Nelson, W. J. (2008). Bench to bedside and back again: molecular mechanisms of alpha-catenin function and roles in tumorigenesis. *Semin. Cancer Biol.* **18**, 53-64.

Berx, G. and van Roy, F. (2009). Involvement of members of the cadherin superfamily in cancer. *Cold Spring Harb. Perspect. Biol.* **1**, a003129.

Berzsenyi, S. and Giangrande, A. (2010). Chain-like cell migration: a collective process conserved throughout evolution. *Trends Dev. Biol.* **4**, 59-68.

Berzsenyi, S., Kumar, A. and Giangrande, A. (2011). Homeostatic interactions at the front of migration control the integrity and the efficiency of a migratory glial chain. *J. Neurosci.* **31**, 13722-13727.

Blagg, S. L. and Insall, R. H. (2004). Solving the WAVE function. *Nat. Cell Biol.* **6**, 279-281.

Brasch, J., Harrison, O. J., Honig, B. and Shapiro, L. (2012). Thinking outside the cell: how cadherins drive adhesion. *Trends Cell Biol.* **22**, 299-310.

Brieher, W. M., Yap, A. S. and Gumbiner, B. M. (1996). Lateral dimerization is required for the homophilic binding activity of C-cadherin. *J. Cell Biol.* **135**, 487-496.

Cafferty, P. and Auld, V. J. (2007). No pun intended: future directions in invertebrate glial cell migration studies. *Neuron Glia Biol.* **3**, 45-54.

Cai, D., Chen, S. C., Prasad, M., He, L., Wang, X., Choesmel-Cadamuro, V., Sawyer, J. K., Danuser, G. and Montell, D. J. (2014). Mechanical feedback through E-cadherin promotes direction sensing during collective cell migration. *Cell* **157**, 1146-1159.

Caussinus, E., Colombelli, J. and Affolter, M. (2008). Tip-cell migration controls stalk-cell intercalation during Drosophila tracheal tube elongation. *Curr. Biol.* **18**, 1727-1734.

Cayre, M., Canoll, P. and Goldman, J. E. (2009). Cell migration in the normal and pathological postnatal mammalian brain. *Prog. Neurobiol.* **88**, 41-63.

Chu, Y. S., Eder, O., Thomas, W. A., Simcha, I., Pincet, F., Ben-Ze'ev, A., Perez, E., Thiery, J. P. and Dufour, S. (2006). Prototypical type I E-cadherin and type II cadherin-7 mediate very distinct adhesiveness through their extracellular domains. *J. Biol. Chem.* **281**, 2901-2910.

Doyle, A. D., Petrie, R. J., Kutys, M. L. and Yamada, K. M. (2013). Dimensions in cell migration. *Curr. Opin. Cell Biol.* **25**, 642-649.

Drees, F., Pokutta, S., Yamada, S., Nelson, W. J. and Weis, W. I. (2005). Alpha-catenin is a molecular switch that binds E-cadherin-beta-catenin and regulates actin-filament assembly. *Cell* **123**, 903-915.

El Sayegh, T. Y., Kapus, A. and McCulloch, C. A. (2007). Beyond the epithelium: cadherin function in fibrous connective tissues. *FEBS Lett.* **581**, 167-174.

Foty, R. A. and Steinberg, M. S. (2004). Cadherin-mediated cell-cell adhesion and tissue segregation in relation to malignancy. *Int. J. Dev. Biol.* **48**, 397-409.

Fung, S., Wang, F., Chase, M., Godt, D. and Hartenstein, V. (2008). Expression profile of the cadherin family in the developing Drosophila brain. *J. Comp. Neurol.* **506**, 469-488.

Galy, A., Schenck, A., Sahin, H. B., Qurashi, A., Sahel, J. A., Diebold, C. and Giangrande, A. (2011). CYFIP dependent actin remodeling controls specific aspects of Drosophila eye morphogenesis. *Dev. Biol.* **359**, 37-46.

Gervais, L. and Casanova, J. (2011). The Drosophila homologue of SRF acts as a boosting mechanism to sustain FGF-induced terminal branching in the tracheal system. *Development* **138**, 1269-1274.

Giagtzoglou, N., Ly, C. V. and Bellen, H. J. (2009). Cell adhesion, the backbone of the synapse: ''vertebrate'' and ''invertebrate'' perspectives. *Cold Spring Harb. Perspect. Biol.* **1**, a003079.

Giangrande, A., Murray, M. A. and Palka, J. (1993). Development and organization of glial cells in the peripheral nervous system of Drosophila melanogaster. *Development* **117**, 895-904.

Gilmour, D. T., Maischein, H. M. and Nüsslein-Volhard, C. (2002). Migration and function of a glial subtype in the vertebrate peripheral nervous system. *Neuron* **34**, 577-588.

Godt, D. and Tepass, U. (2009). Breaking a temporal barrier: signalling crosstalk regulates the initiation of border cell migration. *Nat. Cell Biol.* **11**, 536-538.

Goichberg, P., Shtutman, M., Ben-Ze'ev, A. and Geiger, B. (2001). Recruitment of beta-catenin to cadherin-mediated intercellular adhesions is involved in myogenic induction. *J. Cell Sci.* **114**, 1309-1319.

Gupta, T. and Giangrande, A. (2014). Collective cell migration: ''all for one and one for all''. *J. Neurogenet.* **28**, 190-198.

Halter, D. A., Urban, J., Rickert, C., Ner, S. S., Ito, K., Travers, A. A. and Technau, G. M. (1995). The homeobox gene repo is required for the differentiation and maintenance of glia function in the embryonic nervous system of Drosophila melanogaster. *Development* **121**, 317-332.

Harris, T. J. and Tepass, U. (2010). Adherens junctions: from molecules to morphogenesis. *Nat. Rev. Mol. Cell Biol.* **11**, 502-514.

Hegedüs, B., Marga, F., Jakab, K., Sharpe-Timms, K. L. and Forgacs, G. (2006). The interplay of cell-cell and cell-matrix interactions in the invasive properties of brain tumors. *Biophys. J.* **91**, 2708-2716.

Iwai, Y., Usui, T., Hirano, S., Steward, R., Takeichi, M. and Uemura, T. (1997). Axon patterning requires DN-cadherin, a novel neuronal adhesion receptor, in the Drosophila embryonic CNS. *Neuron* **19**, 77-89.

Iwai, Y., Hirota, Y., Ozaki, K., Okano, H., Takeichi, M. and Uemura, T. (2002). DN-cadherin is required for spatial arrangement of nerve terminals and ultrastructural organization of synapses. *Mol. Cell. Neurosci.* **19**, 375-388.

Kiryushko, D., Berezin, V. and Bock, E. (2004). Regulators of neurite outgrowth: role of cell adhesion molecules. *Ann. N. Y. Acad. Sci.* **1014**, 140-154.

Klämbt, C. (2009). Modes and regulation of glial migration in vertebrates and invertebrates. *Nat. Rev. Neurosci.* **10**, 769-779.

Kobielak, A. and Fuchs, E. (2004). Alpha-catenin: at the junction of intercellular adhesion and actin dynamics. *Nat. Rev. Mol. Cell Biol.* **5**, 614-625.

Kolotuev, I., Schwab, Y. and Labouesse, M. (2010). A precise and rapid mapping protocol for correlative light and electron microscopy of small invertebrate organisms. *Biol. Cell* **102**, 121-132.

Koussa, M. A., Tolbert, L. P. and Oland, L. A. (2010). Development of a glial network in the olfactory nerve: role of calcium and neuronal activity. *Neuron Glia Biol.* **6**, 245-261.

Kurusu, M., Katsuki, T., Zinn, K. and Suzuki, E. (2012). Developmental changes in expression, subcellular distribution, and function of Drosophila N-cadherin, guided by a cell-intrinsic program during neuronal differentiation. *Dev. Biol.* **366**, 204-217.

Lee, B. P. and Jones, B. W. (2005). Transcriptional regulation of the Drosophila glial gene repo. *Mech. Dev.* **122**, 849-862.

Lee, T. and Luo, L. (2001). Mosaic analysis with a repressible cell marker (MARCM) for Drosophila neural development. *Trends Neurosci.* **24**, 251-254.

Lemke, G. (2001). Glial control of neuronal development. *Annu. Rev. Neurosci.* **24**, 87-105.

Marín, O., Valiente, M., Ge, X. and Tsai, L. H. (2010). Guiding neuronal cell migrations. *Cold Spring Harb. Perspect. Biol.* **2**, a001834.

Meyer, S., Schmidt, I. and Klämbt, C. (2014). Glia ECM interactions are required to shape the Drosophila nervous system. *Mech. Dev.* **133**, 105-116.

Montell, D. J. (2003). Border-cell migration: the race is on. *Nat. Rev. Mol. Cell Biol.* **4**, 13-24.

Montell, D. J., Yoon, W. H. and Starz-Gaiano, M. (2012). Group choreography: mechanisms orchestrating the collective movement of border cells. *Nat. Rev. Mol. Cell Biol.* **13**, 631-645.

Murray, M. A., Schubiger, M. and Palka, J. (1984). Neuron differentiation and axon growth in the developing wing of Drosophila melanogaster. *Dev. Biol.* **104**, 259-273.

Näthke, I. S., Hinck, L., Swedlow, J. R., Papkoff, J. and Nelson, W. J. (1994). Defining interactions and distributions of cadherin and catenin complexes in polarized epithelial cells. *J. Cell Biol.* **125**, 1341-1352.

Nelson, W. J. (2008). Regulation of cell-cell adhesion by the cadherin-catenin complex. *Biochem. Soc. Trans.* **36**, 149-155.

Niessen, C. M. and Gottardi, C. J. (2008). Molecular components of the adherens junction. *Biochim. Biophys. Acta* **1778**, 562-571.

Nose, A., Nagafuchi, A. and Takeichi, M. (1988). Expressed recombinant cadherins mediate cell sorting in model systems. *Cell* **54**, 993-1001.

Oda, H., Uemura, T., Shiomi, K., Nagafuchi, A., Tsukita, S. and Takeichi, M. (1993). Identification of a Drosophila homologue of alpha-catenin and its association with the armadillo protein. *J. Cell Biol.* **121**, 1133-1140.

Orsulic, S., Huber, O., Aberle, H., Arnold, S. and Kemler, R. (1999). E-cadherin binding prevents beta-catenin nuclear localization and beta-catenin/LEF-1-mediated transactivation. *J. Cell Sci.* **112**, 1237-1245.

Pacquelet, A. and Rørth, P. (2005). Regulatory mechanisms required for DE-cadherin function in cell migration and other types of adhesion. *J. Cell Biol.* **170**, 803-812.

Pai, L. M., Orsulic, S., Bejsovec, A. and Peifer, M. (1997). Negative regulation of Armadillo, a Wingless effector in Drosophila. *Development* **124**, 2255-2266.

Péglion, F. and Etienne-Manneville, S. (2012). N-cadherin expression level as a critical indicator of invasion in non-epithelial tumors. *Cell Adh. Migr.* **6**, 327-332.

Peifer, M., Sweeton, D., Casey, M. and Wieschaus, E. (1994). wingless signal and Zeste-white 3 kinase trigger opposing changes in the intracellular distribution of Armadillo. *Development* **120**, 369-380.

Rappl, A., Piontek, G. and Schlegel, J. (2008). EGFR-dependent migration of glial cells is mediated by reorganisation of N-cadherin. *J. Cell Sci.* **121**, 4089-4097.
Rieger, S., Senghaas, N., Walch, A. and Köster, R. W. (2009). Cadherin-2 controls directional chain migration of cerebellar granule neurons. *PLoS Biol.* **7**, e1000240.
Rimm, D. L., Koslov, E. R., Kebriaei, P., Cianci, C. D. and Morrow, J. S. (1995). Alpha 1(E)-catenin is an actin-binding and -bundling protein mediating the attachment of F-actin to the membrane adhesion complex. *Proc. Natl. Acad. Sci. USA* **92**, 8813-8817.
Rørth, P. (2003). Communication by touch: role of cellular extensions in complex animals. *Cell* **112**, 595-598.
Rørth, P. (2009). Collective cell migration. *Annu. Rev. Cell Dev. Biol.* **25**, 407-429.
Rotty, J. D., Wu, C. and Bear, J. E. (2013). New insights into the regulation and cellular functions of the ARP2/3 complex. *Nat. Rev. Mol. Cell Biol.* **14**, 7-12.
Sanson, B., White, P. and Vincent, J. P. (1996). Uncoupling cadherin-based adhesion from wingless signalling in Drosophila. *Nature* **383**, 627-630.
Schenck, A., Bardoni, B., Langmann, C., Harden, N., Mandel, J. L. and Giangrande, A. (2003). CYFIP/Sra-1 controls neuronal connectivity in Drosophila and links the Rac1 GTPase pathway to the fragile X protein. *Neuron* **38**, 887-898.
Schenck, A., Qurashi, A., Carrera, P., Bardoni, B., Diebold, C., Schejter, E., Mandel, J. L. and Giangrande, A. (2004). WAVE/SCAR, a multifunctional complex coordinating different aspects of neuronal connectivity. *Dev. Biol.* **274**, 260-270.
Schwabe, T., Gontang, A. C. and Clandinin, T. R. (2009). More than just glue: the diverse roles of cell adhesion molecules in the Drosophila nervous system. *Cell Adh. Migr.* **3**, 36-42.
Shan, W. S., Tanaka, H., Phillips, G. R., Arndt, K., Yoshida, M., Colman, D. R. and Shapiro, L. (2000). Functional cis-heterodimers of N- and R-cadherins. *J. Cell Biol.* **148**, 579-590.
Shapiro, L. and Weis, W. I. (2009). Structure and biochemistry of cadherins and catenins. *Cold Spring Harb. Perspect. Biol.* **1**, a003053.
Silies, M. and Klämbt, C. (2010a). APC/C(Fzr/Cdh1)-dependent regulation of cell adhesion controls glial migration in the Drosophila PNS. *Nat. Neurosci.* **13**, 1357-1364.
Sofroniew, M. V. and Vinters, H. V. (2010). Astrocytes: biology and pathology. *Acta Neuropathol.* **119**, 7-35.
Soustelle, L., Aigouy, B., Asensio, M. L. and Giangrande, A. (2008). UV laser mediated cell selective destruction by confocal microscopy. *Neural Dev.* **3**, 11.
Stepniak, E., Radice, G. L. and Vasioukhin, V. (2009). Adhesive and signaling functions of cadherins and catenins in vertebrate development. *Cold Spring Harb. Perspect. Biol.* **1**, a002949.
Stradal, T. E., Rottner, K., Disanza, A., Confalonieri, S., Innocenti, M. and Scita, G. (2004). Regulation of actin dynamics by WASP and WAVE family proteins. *Trends Cell Biol.* **14**, 303-311.
Tepass, U., Truong, K., Godt, D., Ikura, M. and Peifer, M. (2000). Cadherins in embryonic and neural morphogenesis. *Nat. Rev. Mol. Cell Biol.* **1**, 91-100.
Togashi, H., Sakisaka, T. and Takai, Y. (2009). Cell adhesion molecules in the central nervous system. *Cell Adh. Migr.* **3**, 29-35.
Uchida, N., Honjo, Y., Johnson, K. R., Wheelock, M. J. and Takeichi, M. (1996). The catenin/cadherin adhesion system is localized in synaptic junctions bordering transmitter release zones. *J. Cell Biol.* **135**, 767-779.
Utsuki, S., Sato, Y., Oka, H., Tsuchiya, B., Suzuki, S. and Fujii, K. (2002). Relationship between the expression of E-, N-cadherins and beta-catenin and tumor grade in astrocytomas. *J. Neurooncol.* **57**, 187-192.
Valiente, M. and Marín, O. (2010). Neuronal migration mechanisms in development and disease. *Curr. Opin. Neurobiol.* **20**, 68-78.
Van De Bor, V., Walther, R. and Giangrande, A. (2000). Some fly sensory organs are gliogenic and require glide/gcm in a precursor that divides symmetrically and produces glial cells. *Development* **127**, 3735-3743.
von Hilchen, C. M., Beckervordersandforth, R. M., Rickert, C., Technau, G. M. and Altenhein, B. (2008). Identity, origin, and migration of peripheral glial cells in the Drosophila embryo. *Mech. Dev.* **125**, 337-352.
von Hilchen, C. M., Bustos, A. E., Giangrande, A., Technau, G. M. and Altenhein, B. (2013). Predetermined embryonic glial cells form the distinct glial sheaths of the Drosophila peripheral nervous system. *Development* **140**, 3657-3668.
Weber, G. F., Bjerke, M. A. and DeSimone, D. W. (2011). Integrins and cadherins join forces to form adhesive networks. *J. Cell Sci.* **124**, 1183-1193.
Xiong, W. C., Okano, H., Patel, N. H., Blendy, J. A. and Montell, C. (1994). repo encodes a glial-specific homeo domain protein required in the Drosophila nervous system. *Genes Dev.* **8**, 981-994.
Yamada, S., Pokutta, S., Drees, F., Weis, W. I. and Nelson, W. J. (2005). Deconstructing the cadherin-catenin-actin complex. *Cell* **123**, 889-901.
Yap, A. S., Brieher, W. M. and Gumbiner, B. M. (1997). Molecular and functional analysis of cadherin-based adherens junctions. *Annu. Rev. Cell Dev. Biol.* **13**, 119-146.
Yonekura, S., Xu, L., Ting, C. Y. and Lee, C. H. (2007). Adhesive but not signaling activity of Drosophila N-cadherin is essential for target selection of photoreceptor afferents. *Dev. Biol.* **304**, 759-770.
Zelhof, A. C. and Hardy, R. W. (2004). WASp is required for the correct temporal morphogenesis of rhabdomere microvilli. *J. Cell Biol.* **164**, 417-426.